

## Activation of PPAR $\alpha$ by Fatty Acid Accumulation Enhances Fatty Acid Degradation and Sulfatide Synthesis

Yang Yang,<sup>1,\*</sup> Yuyao Feng,<sup>1,\*</sup> Xiaowei Zhang,<sup>2</sup> Takero Nakajima,<sup>1</sup> Naoki Tanaka,<sup>1</sup> Eiko Sugiyama,<sup>3</sup> Yuji Kamijo<sup>4</sup> and Toshifumi Aoyama<sup>1</sup>

<sup>1</sup>Department of Metabolic Regulation, Shinshu University Graduate School of Medicine, Matsumoto, Nagano, Japan

<sup>2</sup>Department of Neurosurgery, The Second Hospital of Hebei Medical University, Shijiazhuang, Hebei, China

<sup>3</sup>Department of Nutritional Science, Nagano Prefectural College, Nagano, Nagano, Japan

<sup>4</sup>Department of Nephrology, Shinshu University School of Medicine, Matsumoto, Nagano, Japan

Very-long-chain acyl-CoA dehydrogenase (VLCAD) catalyzes the first reaction in the mitochondrial fatty acid  $\beta$ -oxidation pathway. VLCAD deficiency is associated with the accumulation of fat in multiple organs and tissues, which results in specific clinical features including cardiomyopathy, cardiomegaly, muscle weakness, and hepatic dysfunction in infants. We speculated that the abnormal fatty acid metabolism in VLCAD-deficient individuals might cause cell necrosis by fatty acid toxicity. The accumulation of fatty acids may activate peroxisome proliferator-activated receptor (PPAR), a master regulator of fatty acid metabolism and a potent nuclear receptor for free fatty acids. We examined six skin fibroblast lines, derived from VLCAD-deficient patients and identified fatty acid accumulation and PPAR $\alpha$  activation in these cell lines. We then found that the expression levels of three enzymes involved in fatty acid degradation, including long-chain acyl-CoA synthetase (LACS), were increased in a PPAR $\alpha$ -dependent manner. This increased expression of LACS might enhance the fatty acyl-CoA supply to fatty acid degradation and sulfatide synthesis pathways. In fact, the first and last reactions in the sulfatide synthesis pathway are regulated by PPAR $\alpha$ . Therefore, we also measured the expression levels of enzymes involved in sulfatide metabolism and the regulation of cellular sulfatide content. The levels of these enzymes and cellular sulfatide content both increased in a PPAR $\alpha$ -dependent manner. These results indicate that PPAR $\alpha$  activation plays defensive and compensative roles by reducing cellular toxicity associated with fatty acids and sulfuric acid.

**Keywords:** cerebroside sulfotransferase; peroxisome proliferator-activated receptor  $\alpha$ ; serine palmitoyl-CoA transferase; sulfatides; very-long-chain acyl-CoA dehydrogenase

Tohoku J. Exp. Med., 2016 October, 240 (2), 113-122. © 2016 Tohoku University Medical Press

### Introduction

Mitochondrial acyl-CoA dehydrogenases catalyze the first reaction of the fatty acid  $\beta$ -oxidation pathway, converting acyl-CoA to enoyl-CoA. These dehydrogenases comprise four isozymes: short-chain acyl-CoA dehydrogenase (SCAD), medium-chain acyl-CoA dehydrogenase (MCAD), long-chain acyl-CoA dehydrogenase (LCAD), and very-long-chain acyl-CoA dehydrogenase (VLCAD), which have overlapping substrate specificity (Izai et al. 1992; Aoyama et al. 1994). VLCAD and LCAD catalyze reactions that generate long-chain fatty acyl-CoAs such as palmitoyl-CoA. Notably, VLCAD contributes more than 90% of palmitoyl-CoA dehydrogenation activity in human heart and liver tissue (Aoyama et al. 1995b). VLCAD deficiency is associated with the accumulation of fat in multiple organs

and tissues, liver dysfunction, cardiomyopathy, cardiomegaly, muscle weakness, and fasting coma with high frequency (Aoyama et al. 1993, 1995a). Additionally, mutation analyses have identified a genotype-phenotype relationship for VLCAD deficiency (Aoyama et al. 1995a; Souri et al. 1996; Andresen et al. 1999; Gregersen et al. 2001). Mutation analysis of six patients has revealed homozygous loss of 35 amino acids in patients 1 and 6 (Aoyama et al. 1995a), homozygous loss of glutamate-130 in patient 2 (Souri et al. 1996), point mutation of lysine-382 to glutamine and loss of glutamate-130 in patient 3 (Souri et al. 1996), homozygous loss of lysine-299 in patient 4 (Souri et al. 1996), and loss of 45 amino acids and point mutation of arginine-613 to tryptophan in patient 5 (Souri et al. 1996). Immunoblot analysis using an anti-human VLCAD antibody demonstrated the absence of mature

Received April 18, 2016; revised and accepted September 6, 2016. Published online September 17, 2016; doi: 10.1620/tjem.240.113.

\*These two authors contributed equally to this work.

Correspondence: Yuji Kamijo, M.D., Ph.D., Department of Nephrology, Shinshu University School of Medicine, 3-1-1 Asahi, Matsumoto, Nagano 390-8621, Japan.

e-mail: yujibeat@shinshu-u.ac.jp

VLCAD protein in all cell lines (Aoyama et al. 1995b). Consequently, these six patients all exhibited severe VLCAD deficiency.

We speculated that long-chain fatty acids and their derivatives could accumulate in multiple tissues and organs in VLCAD-deficient patients. In turn, the resulting fatty acid toxicity may trigger cell necrosis in the liver, heart, and skeletal muscle (Aoyama et al. 1995b). This potential accumulation of long-chain fatty acids could activate peroxisome proliferator-activated receptors (PPARs), a group of nuclear receptors, as their endogenous ligands (Forman et al. 1997; Kliewer et al. 1997) to enhance fatty acid degradation (Aoyama et al. 1998). Additionally, this fatty acid accumulation might increase the supply of palmitoyl-CoA, a representative long-chain fatty acid ester, and other long-chain fatty acid derivatives involved in ceramide/sphingolipid synthesis. Here, we have focused our attention on sulfatides, which are specific and ubiquitous glycosphingolipids built from ceramide, galactose, and sulfate (Fig. 1) (Nakajima et al. 2013). This is because the two possible rate-limiting reactions catalyzed by serine palmitoyl-CoA transferase (SPT) and cerebroside sulfotransferase (CST) in the sulfatide synthesis pathway (Fig. 1) are potentially regulated through PPAR in rodents (Rivier et al. 2000; Baranowski et al. 2007; Zabielski et al. 2010; Yamane et al. 2011; Kimura et al. 2012; Nakajima et al. 2013). Our study also investigates the control mechanisms involved in human sulfatide metabolism, which are currently unknown. We have examined fatty acid accumulation, PPAR activation, and changes in the metabolic regulation of fatty acids and sulfatides using VLCAD-deficient cells.

## Materials and Methods

### *Source of VLCAD-deficient skin fibroblasts and culture method*

The case histories of six VLCAD patients were reported previously (Aoyama et al. 1993, 1995b). Patients 1 and 3 were female while the others were male (Aoyama et al. 1995b). Skin tissues were collected from each of the six patients and skin fibroblasts were cultured in Dulbecco's modified Eagle's medium containing 10% (*v/v*) fetal calf serum, 1× antibiotic-antimycotic solution (Invitrogen Life Technologies Corp., Carlsbad, CA, USA), 0.1 mM nonessential amino acids, and 4.5 mg D-glucose/mL. Skin tissues were also collected from three healthy adult men and skin fibroblasts were cultured as described previously (Aoyama et al. 1995b).

### *Chemicals*

MK886, a PPAR $\alpha$ -specific antagonist (Kehrer et al. 2001), and fenofibrate (FF) were obtained from Wako Pure Chemical (Osaka, Japan) and Sigma Chemical Company (St. Louis, MO, USA), respectively.

### *Analyses of free fatty acids (FFA) and triglycerides (TG)*

To determine the content of FFA and TG, 20–30 mg of pelleted cells was mixed with 150  $\mu$ L cold water. The mixture was treated with a microsonicator (Powersonic Model 50, Yamato, Tokyo, Japan) (Aoyama et al. 1990; Nakajima et al. 1994), and lipids were extracted with 18 volumes of *n*-hexane/isopropanol solution (3:2, *v/v*) as

described previously (Li et al. 2007). Impurities in the lipid fraction were removed by washing with aqueous sodium sulfate (Nakajima et al. 1994; Li et al. 2007). The amounts of FFA and TG were measured using an NEFA C-test kit and a triglyceride E-test kit (Wako Pure Chemical, Osaka, Japan), respectively.

### *Octanoyl-CoA dehydrogenase activity*

Because the assay using electron transfer flavoprotein (Furuta et al. 1981) is more sensitive and reliable than that using ferricinium ion (Lehman et al. 1990), the former was adopted in this study. Briefly, approximately 3 mg of pelleted cells was resuspended in 150  $\mu$ L of solution containing 67 mM potassium phosphate (pH 7.5), 200 mM sodium chloride, and 0.6% (*w/v*) Triton X-100. The suspension was gently sonicated, and the solution was centrifuged at 3,000  $\times$  g for 5 min. Fifty  $\mu$ L of the supernatant fraction was mixed with a solution containing 67 mM potassium phosphate (pH 7.5), 50  $\mu$ M octanoyl-CoA, and 0.4  $\mu$ M electron transfer flavoprotein in a final volume of 1.5 mL. The mixture without the electron transfer flavoprotein was preincubated for 2 min at 37°C with gentle bubbling of nitrogen gas to exclude oxygen. The reaction was started by addition of the electron transfer flavoprotein, and carried out under nitrogen gas. Electron transfer flavoprotein reduction was measured by using a fluorometer (Hitachi F-2000, Hitachi High-Tech Science Co., Tokyo, Japan) with excitation at 342 nm and emission at 496 nm.

### *Assays for DNA-binding activity of PPARs*

The DNA-binding activities of PPAR $\alpha$ , PPAR $\delta$ , and PPAR $\gamma$  were determined using the PPAR $\alpha$ , PPAR $\delta$ , and PPAR $\gamma$  Transcription Factor Assay kits (Cayman Chemical, Ann Arbor, MI, USA), respectively. These assays are based on an enzyme-linked immunosorbent assay using PPAR response element (PPRE)-immobilized microplates and specific PPAR antibodies, thus offering similar results to those of the conventional radioactive electrophoretic mobility shift assay. DNA-binding assays were carried out according to the manufacturer's instructions using whole cell lysates (100  $\mu$ g protein per assay). An equal weight of cells from the individual patient or control were mixed and used. Results are expressed as the fold-change relative to the control cells.

### *Immunoblot analysis*

Whole cell lysates (60  $\mu$ g protein) were subjected to 10% SDS-polyacrylamide gel electrophoresis. After electrophoresis, proteins were transferred to polyvinylidene fluoride membranes (GE Healthcare, Little Chalfont, UK), which were incubated with the primary antibody and then with alkaline phosphatase-conjugated goat anti-rabbit IgG (Aoyama et al. 1989, 1990). Antibodies specific for LCAD, MCAD, and long-chain acyl-CoA synthetase (LACS) were described previously (Aoyama et al. 1998). Actin protein levels served as the loading control. Band intensities were measured by densitometry, normalized to those of actin, and then expressed as fold-changes relative to the average value of the three control cells.

### *Extraction and measurement of sulfatides*

An equal weight of cells from an individual patient or control was mixed and used. The sample (20 mg) was treated with a microsonicator (Powersonic Model 50) in 6 volumes of cold water, and lipids were extracted with 18 volumes of *n*-hexane/isopropanol solution (3:2, *v/v*), as described previously (Li et al. 2007). Lipid extracts were then treated with methanolic sodium hydroxide to convert sulfa-

tides to their corresponding lysosulfatides (LS; sulfatides without fatty acids) (Li et al. 2007). After purification through Mono-tip C18 cartridges (GL Sciences, Tokyo, Japan), LS samples were analyzed by matrix-assisted laser desorption ionization-time of flight mass spectrometry (MALDI-TOF MS) together with *N*-acetylated LS-sphinganine (d18:0) as the internal standard (Li et al. 2007). MS analyses were performed on a TOF/TOF 5800 system (AB Sciex, Framingham, MA, USA) using a negative ion reflector mode with two-point external calibration: *N*-acetylated LS-d18:0 ( $[M-H]^-$  584.310) and LS-(4*E*)-sphinganine (d18:1) ( $[M-H]^-$  540.284). Five molecular species of LS were detected as follows: LS-sphingadienine (d18:2), LS-d18:1, LS-d18:0, LS-icosasphinganine (d20:0), and LS-4D-hydroxyicosasphinganine (t20:0). LS-4D-hydroxyicosasphinganine (t18:0) and LS-(4*E*)-icosasphinganine (d20:1) were undetected (Hu et al. 2007; Li et al. 2007). The total amount of sulfatides in each sample was calculated as the sum of these five LS species.

#### Analysis of mRNA

An equal weight of cells from an individual patient or control

was mixed and used. Total RNA was extracted using an RNeasy Mini Kit (QIAGEN, Hilden, Germany), and samples of 2  $\mu$ g of RNA were reverse-transcribed using oligo-dT primers and SuperScript II reverse transcriptase (Invitrogen Life Technologies Corp.). The mRNA levels were quantified by real-time polymerase chain reaction using a SYBR Premix Ex Taq™ II (Takara Bio, Otsu, Japan) on a Thermal Cycler Dice TP800 system (Takara Bio) (Kamijo et al. 2007; Kanbe et al. 2014). Specific primers were designed using Primer Express Software 2.0 (Applied Biosystems, Foster City, CA, USA) (Table 1). The mRNA levels of glyceraldehyde-3-phosphate dehydrogenase (*GAPDH*, gene encoding human GAPDH) were used as an internal control. Measurements of mRNA levels were normalized to those of *GAPDH* and then expressed as fold-changes relative to the average value of the three controls.

#### Statistical analysis

All data are expressed as the mean  $\pm$  standard deviation (SD). Statistical analyses were performed using one-way ANOVA or two-way ANOVA with Bonferroni correction (SPSS Statistics 17.0; SPSS

Table 1. Primer pairs used for real-time PCR.

Gene	GenBank accession number		Primer sequence (5' to 3')
<i>ACADL</i>	NM_001608	F	TCACTCAGAATGGGAGAAAGC
		R	CTCCAATTCCACCAAGATGCT
<i>ACADM</i>	NM_000016	F	TAACCAACGGAGGAAAAGCT
		R	CTGCTTCCACAATGAATCCA
<i>ACSL1</i>	NM_001995	F	AACAGACGGAAGCCCAAGC
		R	TCGGTGAGTGACCATTGCTC
<i>ARSA</i>	NM_000487	F	TATGCCTCTCACCACAC
		R	GGTCTCAGGTCCATTGTC
<i>GAL3ST1</i>	NM_004861	F	GAAGACGCACAAGACGGCCA
		R	AAGGCGAACTTGAGCCGGTG
<i>GALC</i>	NM_000153	F	GCAACCTCCCGACTTCTAGTA
		R	ACCACTCGTATCCTCGGAAATA
<i>GAPDH</i>	NM_002046	F	CCTCAAGATCATCAGCAATGC
		R	GGTCATGAGTCCTTCCACGAT
<i>PPARA</i>	NM_005036	F	GCCGAGCTCCAAGCTACTCT
		R	CAACAGTTTGTGGCAAGACAA
<i>PPARD</i>	NM_006238	F	ATCTGACCCTGCTTTCCAGA
		R	TCACACAGTGGCTTCTGCTC
<i>PPARG</i>	NM_005037	F	CGGAGCTGATCCCAAAGTT
		R	CTCGAGGACACCGGAGAG
<i>SPTLC1</i>	NM_006415	F	TGAAGGAAAAGTGCGGACA
		R	TGTAGGTGAAAAGGCTGGAGA
<i>SPTLC2</i>	NM_004863	F	GAGTCCAGAGCCAGGTTTTG
		R	CTGAGGGAGCACCAAAAAG
<i>SPTLC3</i>	NM_018327	F	ACCGATAGCAGAGCAAATCA
		R	TTCGCAAGTTGCTGTACTCTC
<i>UGT8</i>	NM_003360	F	CAAACCAGCCAGCCACTACCAGAA
		R	TTCTAGATTCTTTGGTTGGGTCC

F, forward sequence; R, reverse sequence.

Inc., Chicago, IL, USA). Correlation coefficients were calculated using Spearman's rank correlation analysis. A probability value of less than 0.05 was considered to be statistically significant.

## Results

### Analyses of FFA and TG

Six strains of skin fibroblasts from VLCAD-deficient patients and three strains from healthy adult men were prepared as described above. The doubling times for these cell strains were approximately 4.5-5.5 days, with no significant differences among the cell strains. VLCAD deficiency impairs the first reaction in the mitochondrial fatty acid  $\beta$ -oxidation pathway. Therefore, increased levels of FFA, TG, and fatty acyl-CoAs were expected to be present. The

levels of FFA and TG were measured first, because simple and conventional assay kits were available. The FFA content of patient cells was 2.9-fold higher than that of control cells (Fig. 2A). TG levels ranged from 20-110  $\mu\text{g/g}$ , with wide differences among individuals and thus there was no statistically significant difference between the patients' and control cells under the culture conditions adopted. These FFA and TG levels were much lower than those present in human serum.

### Assays for DNA-binding activity of PPARs

We next investigated whether the increased levels of FFA in patient cells activated PPAR by serving as a source of endogenous ligands (Forman et al. 1997; Kliewer et al.

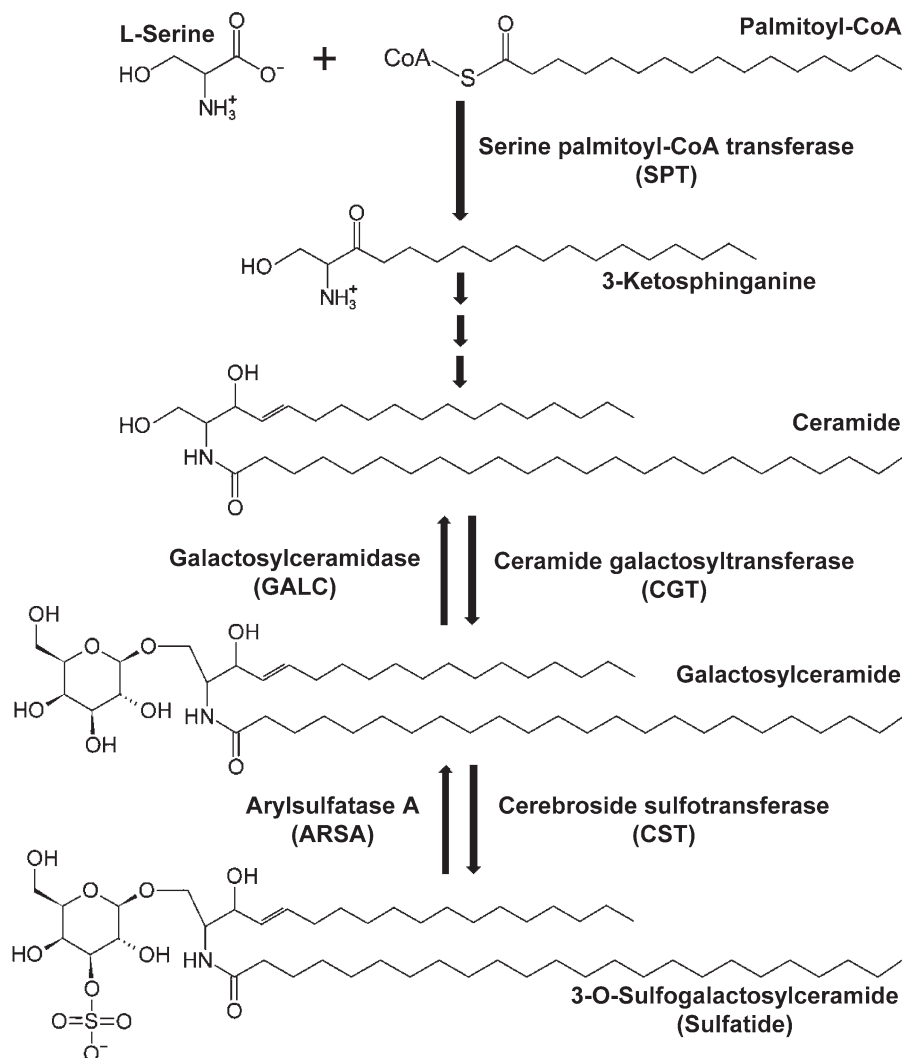


Fig. 1. Simple metabolic pathway of sulfatide metabolism.

The *de novo* synthesis of sphingolipids including sulfatides is initiated by an SPT-catalyzed condensation reaction between L-serine and palmitoyl-CoA. Three additional reactions are required to generate ceramides, the common intermediate molecules in sphingolipid synthesis. Sulfatides are synthesized from ceramides through galactosylceramides in reactions catalyzed by CGT in the endoplasmic reticulum and CST in Golgi membranes. During degradation, sulfatides are first subjected to a desulfation reaction mediated by ARSA, followed by deglycosylation through GALC, resulting in reproduction of ceramides. Chemical examples shown in this figure possess a d18:1 sphingoid base structure with a C24:0 fatty acid (cerebronic acid) moiety.

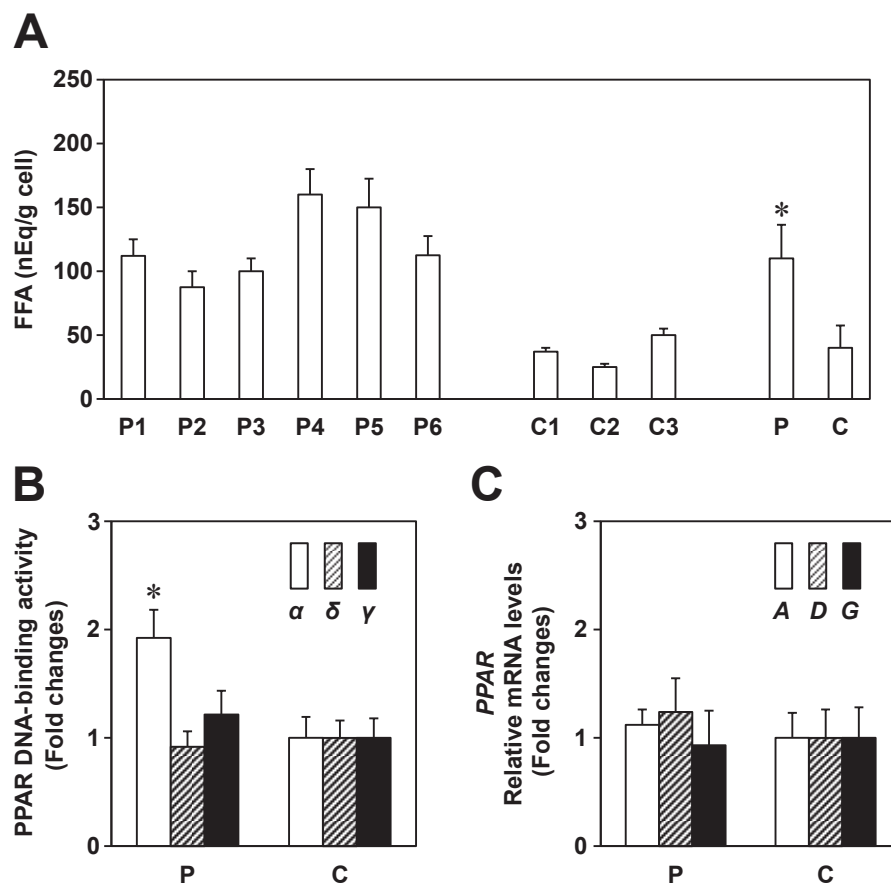


Fig. 2. FFA content, PPAR DNA-binding activity, and expression levels of mRNA encoding *PPARs*. A. Cellular FFA content. P1-P6, individual patient cells; C1-C3, individual control cells; P, mean  $\pm$  SD in cells from six patients; C, mean  $\pm$  SD in three control cells. B. PPAR DNA-binding activity. P, mean  $\pm$  SD in cells from six patients; C, mean  $\pm$  SD in three control cells.  $\alpha$  (open bar), PPAR $\alpha$ ;  $\delta$  (hatched bar), PPAR $\delta$ ;  $\gamma$  (closed bar), PPAR $\gamma$ . C. Relative *PPAR* mRNA levels. A (open bar), *PPARA*, gene encoding human PPAR $\alpha$ ; D (hatched bar), *PPARD*, gene encoding human PPAR $\delta$ ; G (closed bar), *PPARG*, gene encoding human PPAR $\gamma$ . \* $P < 0.05$  versus controls. Statistical analysis was performed using one-way ANOVA.

1997). PPAR activation was examined together with levels of PPAR mRNA expression. The PPAR DNA-binding assay revealed a 1.9-fold higher activity of PPAR $\alpha$  in whole-cell lysates from the patient cells (Fig. 2B). There were no changes in the mRNA expression levels of the three species of PPAR between patient and control cells (Fig. 2C). Additionally, real-time quantitative PCR revealed that the relative mRNA levels of PPAR $\alpha$  (*PPARA*), PPAR $\delta$  (*PPARD*), and PPAR $\gamma$  (*PPARG*) in the control cells were  $0.3 \times 10^{-1}$ ,  $0.1 \times 10^{-1}$ , and  $0.2 \times 10^{-2}$ , respectively, when compared with the GAPDH (*GAPDH*) mRNA level. The presence of significant PPAR $\alpha$  activation and the absence of PPAR $\gamma$  activation (Fig. 2B) may result from a very low level of PPAR $\gamma$  expression.

#### Protein and mRNA analyses for PPAR $\alpha$ target gene products

We next investigated changes in the expression levels of three typical PPAR $\alpha$  target gene products—LCAD, MCAD, and LACS (Aoyama et al. 1998)—to confirm the

significance of PPAR $\alpha$  activation in patient cells. LCAD and MCAD are involved in the fatty acid degradation pathway, while LACS converts long-chain fatty acids to fatty acyl-CoAs, all of which can reduce fatty acid toxicity. Expression of LCAD protein and its mRNA (*ACADL*) increased in the patient cells, as did the protein and mRNA levels of MCAD (*ACADM*) and LACS (*ACSL1*) (Fig. 3A, B).

#### Octanoyl-CoA dehydrogenase activity

Octanoyl-CoA dehydrogenase activity in patient cells was higher than that in control cells, and this increased activity was reduced by treatment with MK886, a PPAR $\alpha$ -specific antagonist (Kehrer et al. 2001) (Fig. 3C). MK886 treatment did not influence enzyme activity in the control cells (Fig. 3C). These data suggest that functional PPAR $\alpha$  activation likely occurred in VLCAD-deficient cells through the increased levels of FFA, leading to enhanced fatty acid degradation catalyzed by LCAD and MCAD.

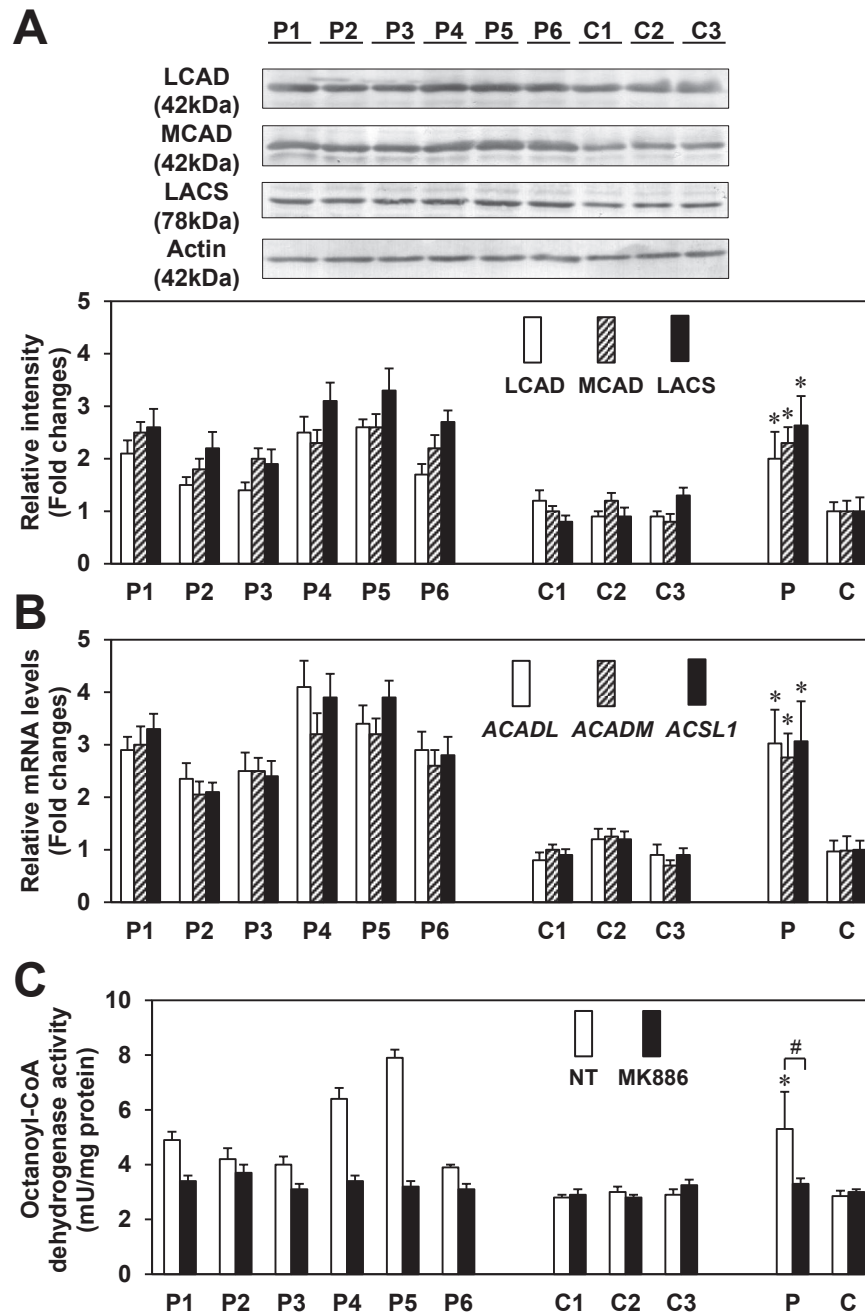


Fig. 3. Expression levels of LCAD, MCAD, and LACS, and octanoyl-CoA dehydrogenase activity.

A. Relative quantification of the expression levels of LCAD, MCAD, and LACS. Upper panel indicates protein bands from immunoblot analysis. Actin was used as the loading control. Lower panel indicates relative protein amounts obtained by immunoblot and densitometric analyses. P1-P6, individual patient cells; C1-C3, individual control cells; P, mean  $\pm$  SD in cells from six patients; C, mean  $\pm$  SD in three control cells. B. Relative mRNA expression. Open bar, *ACADL*, gene encoding human LCAD; hatched bar, *ACADM*, gene encoding human MCAD; closed bar, *ACSL1*, gene encoding human LACS. C Octanoyl-CoA dehydrogenase activity. MK886 treatment is described in the legend for Fig. 4. Open bar, no treatment (NT); closed bar, MK886 treatment. \* $P < 0.05$  versus controls; # $P < 0.05$ , NT versus MK886 treatment. Statistical analysis was performed using two-way ANOVA.

#### Measurement of mRNA levels of enzymes involved in sulfatide metabolism

mRNA expression levels of the five key enzymes involved in sulfatide metabolism (Fig. 1) were analyzed. SPT is particularly important because it is possibly the rate-limiting enzyme in the synthesis of ceramide/sphingolipids

including sulfatides (Hanada 2003). SPT is a heterodimer, comprising subunit LC1 and subunit LC2 or LC3. The expression levels of SPT and the other four enzymes: CST, arylsulfatase A (ARSA), ceramide galactosyltransferase (CGT), and galactosylceramidase (GALC) were investigated using immunoblot analysis. However, it was hard to

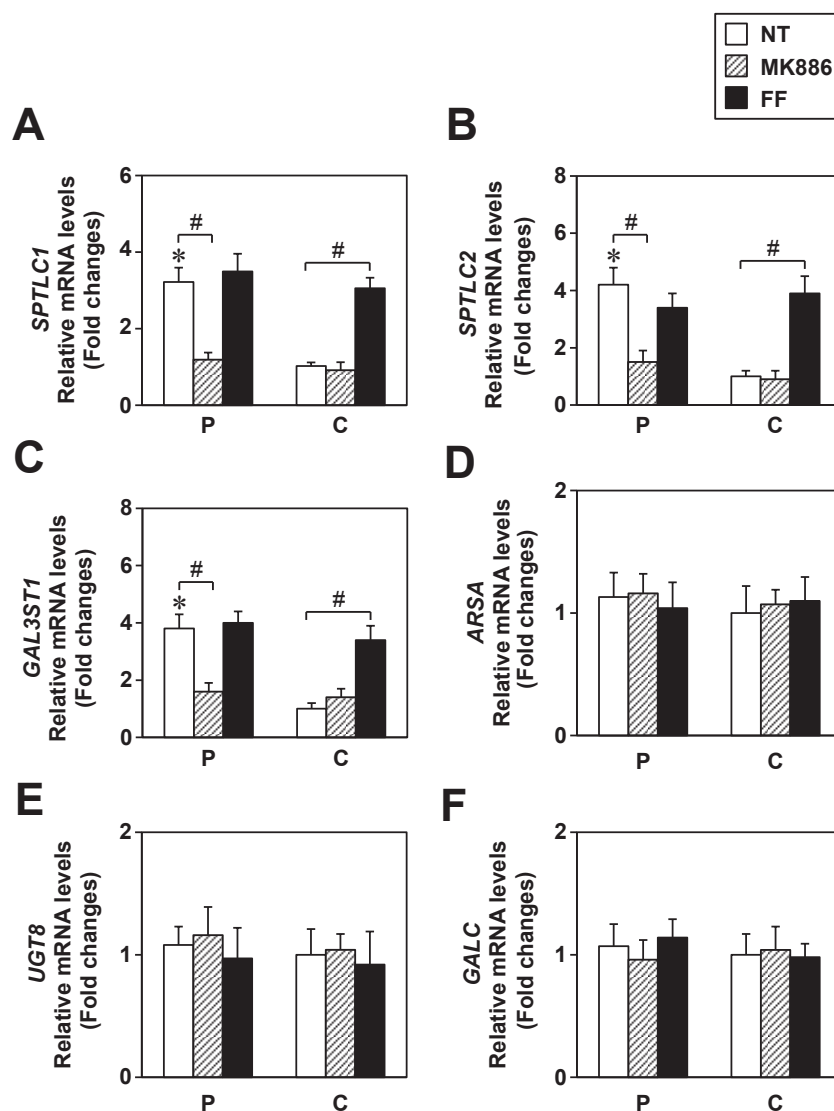


Fig. 4. Effects of MK886 or fenofibrate (FF) treatment on the mRNA expression levels of enzymes involved in sulfatide synthesis and degradation.

Cells were plated in dishes and allowed to grow to 80% confluence. MK886 (30  $\mu$ M final concentration) and FF (200  $\mu$ M final concentration) were added to the cell culture media. Both chemicals were dissolved in DMSO, and the final concentration of DMSO in media was maintained at 0.05% (v/v) in all cases. After 6 h, the cells were harvested and mRNA expression levels measured. mRNA levels were normalized to those of *GAPDH* and are shown as fold changes relative to those of the control. *SPTLC1*, gene encoding human SPT subunit LC1; *SPTLC2*, gene encoding human SPT subunit LC2; *GAL3ST1*, gene encoding human CST; *ARSA*, gene encoding human ARSA; *UGT8*, gene encoding human CGT; *GALC*, gene encoding human GALC. P, mean  $\pm$  SD in cells from six patients; C, mean  $\pm$  SD in three control cells. Open bar, no treatment (NT); hatched bar, MK886 treatment; closed bar, FF treatment. \* $P < 0.05$  versus controls; # $P < 0.05$ , NT versus MK886 or FF treatment. Statistical analysis was performed using two-way ANOVA.

detect a distinctive protein band in all cases because of the poor reactivity of the commercially available primary antibodies against the low content of human proteins in the cell strains. Instead, the expression levels of mRNA were examined. The expression level of *SPTLC1* (*SPTLC1*) mRNA in patient cells was 3.2-fold higher than that in control cells (Fig. 4A). This high level of expression in patient cells was significantly decreased by MK886 treatment but unchanged by treatment with the potent PPAR $\alpha$  agonist, FF, (Fig. 4A). The low level of expression in control cells was unchanged by MK886 treatment and markedly increased by

FF treatment (Fig. 4A). Changes in the expression level of *SPTLC2* (*SPTLC2*) mRNA were similar to those for *SPTLC1* (*SPTLC1*) mRNA (Fig. 4B). The expression level of *SPTLC3* (*SPTLC3*) mRNA was very low in all samples. This suggests that SPT mainly exists as a heterodimer of subunits LC1 and LC2 within cells. The changes in the expression level of CST (*GAL3ST1*) mRNA (Fig. 4C) were similar to those for *SPTLC1* (*SPTLC1*)/*SPTLC2* (*SPTLC2*) mRNA. These data indicate that the expression levels of *SPTLC1*, *SPTLC2*, and CST are highly regulated by PPAR $\alpha$ . The expression levels of ARSA (*ARSA*), CGT

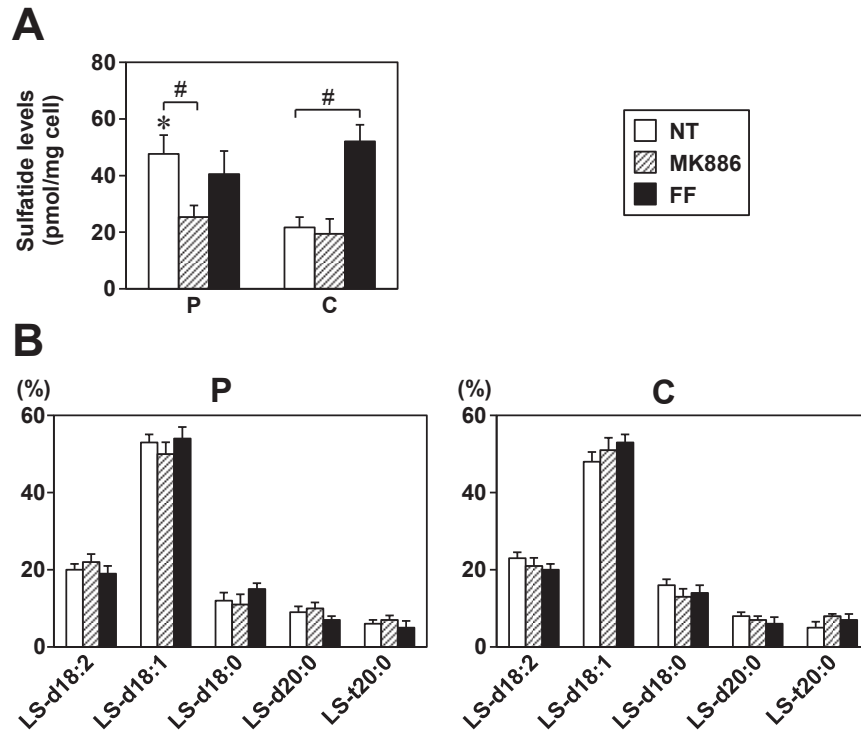


Fig. 5. Effects of MK886 or fenofibrate (FF) treatment on the levels and compositions of sulfatides. A. Sulfatide levels. P, mean  $\pm$  SD in cells from six patients; C, mean  $\pm$  SD in three control cells. The same samples used in Fig. 4 were analyzed. Open bar, no treatment (NT); hatched bar, MK886 treatment; closed bar, FF treatment. \* $P < 0.05$  versus controls; # $P < 0.05$ , NT versus MK886 or FF treatment. B. Percentage content of the five LS molecular species. Each sulfatide content in Fig. 5A indicates the total amount of the individual content of the five LS molecular species, while the individual percentage of each of the five contents is shown in Fig. 5B. Statistical analysis was performed using two-way ANOVA

(*UGT8*), and *GALC* (*GALC*) mRNA were unchanged in all cases (Fig. 4D-F), demonstrating PPAR $\alpha$ -independent gene regulation.

#### Measurement of sulfatides

Sulfatide levels and the sphingoid composition were measured to confirm the changes in mRNA expression levels of the five enzymes involved in sulfatide metabolism. The constitutive sulfatide level in the patient cells was 2.3-fold higher than that in the control cells (Fig. 5A). This higher sulfatide level was decreased by MK886 treatment and unchanged by FF treatment of patient cells (Fig. 5A). The lower sulfatide level was unchanged by MK886 treatment and greatly increased by FF treatment in the control cells (Fig. 5A). These data show that sulfatide levels are significantly regulated by PPAR $\alpha$ , reflecting the regulation of *SPTLC1/2* (*SPTLC1/2*) and *CST* (*GAL3ST1*) mRNA. The sphingoid compositions of sulfatides were similar in all cases (Fig. 5B) and were very different from those in human serum (Hu et al. 2007; Li et al. 2007).

#### Discussion

The severe phenotype of VLCAD deficiency presents as multi-organ dysfunction, with the liver, heart, skeletal muscle, and other organs affected by cell necrosis (Aoyama et al. 1993, 1995b; Gregersen et al. 2001). Here we have

described increased FFA accumulation in the cells of VLCAD-deficient patients. These increased levels of FFA could result in cell toxicity and promote functional PPAR $\alpha$  activation. Functional activation of PPAR $\alpha$  was present only in patient cells, with expression levels of *LACS*, *MCAD*, and *LCAD* consistently upregulated (Aoyama et al. 1998). *MCAD* and *LCAD* function in the elimination of FFA through mitochondrial fatty acid  $\beta$ -oxidation—the pathway responsible for fatty acid degradation—to reduce fatty acid toxicity. Notably, *LCAD* can catalyze reactions that are normally catalyzed by *VLCAD* despite its lower specific activity (Izai et al. 1992). *LACS* catalyzes the conversion of long-chain fatty acids to CoA esters, thereby decreasing fatty acid toxicity and increasing the supply of substrates for fatty acid  $\beta$ -oxidation and ceramide/sphingolipid synthesis. These findings suggest that functional PPAR $\alpha$  activation plays defensive and compensative roles. Furthermore, activation of functional PPAR $\alpha$  also increased sulfatide levels by promoting increased expression of the sulfatide synthesis pathway components *SPT* and *CST*. Sulfatides form sulfuric conjugates by incorporating the sulfuric residue from 3'-phosphoadenosine 5'-phosphosulfate and can be present in cells at very high concentrations. For example, sulfatide levels of approximately 1.5 and 5 nmol/mg tissue have been detected in kidney and brain tissues, respectively, without signs of cell toxicity (Nakajima

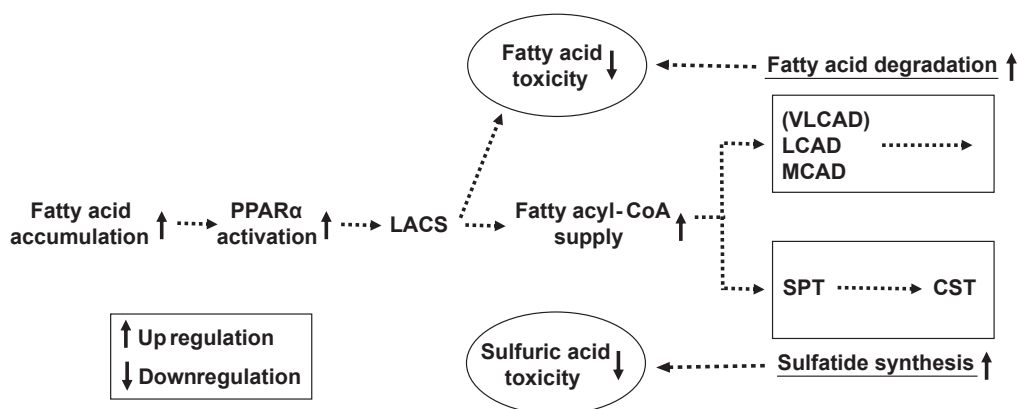


Fig. 6. Scheme relating to the multiple effects of PPAR $\alpha$  activation.

(VLCAD) indicates the absence of VLCAD in the patient. Upper box indicates the mitochondrial fatty acid  $\beta$ -oxidation pathway, which performs fatty acid degradation. The first reaction is catalyzed by LCAD or MCAD for long-chain or medium-chain fatty acyl-CoAs, respectively. Lower box indicates the sulfatide synthesis pathway. The first and the last reactions are catalyzed by SPT and CST, respectively. Expression levels of LACS, LCAD, MCAD, SPT, and CST are all increased by PPAR $\alpha$  activation. The increased expression of LACS enhances fatty acyl-CoA synthesis, which increases the supply of fatty acyl-CoA to both pathways and decreases fatty acid toxicity by converting fatty acids to relevant CoA esters.

et al. 2013). An increased sulfatide level might decrease sulfuric acid toxicity in cells, suggesting another defensive role of functional PPAR $\alpha$  activation. These proposed complicated associations are depicted in Fig. 6. The defensive roles of PPAR $\alpha$  activation might prevent cell necrosis in the organs and tissues of patients with the severe phenotype of VLCAD-deficiency, so administration of PPAR $\alpha$  agonists such as fibrates may prevent and/or relieve complications. Additionally, these patients should consume food containing low amounts of long-chain fatty acids and their derivatives.

This study is the first to demonstrate PPAR $\alpha$ -dependent regulation of human sulfatide metabolism using cells derived from VLCAD-deficient patients with constitutively activated PPAR $\alpha$ . This PPAR $\alpha$  activation enhances expression levels of the two key enzymes in sulfatide synthesis, SPT and CST, and increases sulfatide content without changing the sphingoid composition. The relationship between CST expression and PPAR $\alpha$  activation has been identified in human cells in our present study, and previously in mice (Kimura et al. 2012; Nakajima et al. 2013). However, the relationship between SPT expression and PPAR $\alpha$  remains controversial. For example, administration of Wy-14,643—a potent PPAR $\alpha$  agonist—did not affect the induction of SPT expression in the hearts of rats fed a normal diet, but did induce SPT expression in those fed a high-fat diet (Baranowski et al. 2007). Wy-14,643 treatment enhanced SPT expression and activity in cultured human skin cells, though this increase completely disappeared with long-term culture (Rivier et al. 2000). Additionally, administration of another PPAR $\alpha$  agonist, bezafibrate, negatively affected SPT expression in regenerating rat liver tissue (Zabielski et al. 2010). Meanwhile, feeding with a high-fat diet reduced SPT expression and PPAR $\alpha$  activity in rat skin (Yamane et al.

2011). Indeed, numerous factors influence the relationship between PPAR $\alpha$  and SPT, and further experiments are needed to gain a more complete understanding of this association. Our present study simply suggests that the gene encoding SPT is a target of PPAR $\alpha$  similar to the case for CST in humans. In support, we searched for putative PPAR-binding sites, PPRE, in the promoter regions of the human genes, *SPTLC2*, which encodes the SPT subunit LC2 and *GAL3ST1*, which encodes CST. We used two separate databases, JASPAR (<http://jaspar.genereg.net/>), and ALGGEN (Algorismica i Genetica, <http://algggen.lsi.upc.es/>). This investigation revealed several candidate regions, as follows:  $-5978/-5966$  (5'-GGAGCAGAGGTAA-3'),  $-7570/-7558$  (5'-TTACCTTTACCT-3'),  $-4539/-4527$  (5'-TGACTCTTGACCA-3'), and  $-2935/-2923$  (5'-TAACCTCTGCCTC-3') from exon 1 of *SPTLC2*; and  $-9923/-9911$  (5'-TGCCCCCTCTCCT-3'),  $-7892/-7880$  (5'-AGGGCAAAGATGA-3'),  $-2312/-2300$  (5'-GGGCCAGTGGGCA-3'), and  $-1238/-1226$  (5'-TGCCTCTGCCTC-3') from exon 1 of *GAL3ST1*. This information may guide future *in vitro* experiments to confirm the functional importance of these sites.

### Acknowledgments

We would like to thank Mrs. Chiyoko Aoyama (Rinko Hospital, Kawasaki, Japan) and Mr. Yuichi Aoyama (AOI International Hospital, Kawasaki, Japan) for helpful comments.

### Conflict of Interest

The authors declare no conflict of interest.

### References

- Andresen, B.S., Olpin, S., Poorthuis, B.J., Scholte, H.R., Vianey-Saban, C., Wanders, R., Ijlst, L., Morris, A., Pourfarzam, M., Bartlett, K., Baumgartner, E.R., deKlerk, J.B., Schroeder,

- L.D., Corydon, T.J., Lund, H., et al. (1999) Clear correlation of genotype with disease phenotype in very-long-chain acyl-CoA dehydrogenase deficiency. *Am. J. Hum. Genet.*, **64**, 479-494.
- Aoyama, T., Hardwick, J.P., Imaoka, S., Funae, Y., Gelboin, H.V. & Gonzalez, F.J. (1990) Clofibrate-inducible rat hepatic P450s IVA1 and IVA3 catalyze the omega- and (omega-1)-hydroxylation of fatty acids and the omega-hydroxylation of prostaglandins E<sub>1</sub> and F<sub>2α</sub>. *J. Lipid Res.*, **31**, 1477-1482.
- Aoyama, T., Peters, J.M., Iritani, N., Nakajima, T., Furihata, K., Hashimoto, T. & Gonzalez, F.J. (1998) Altered constitutive expression of fatty acid-metabolizing enzymes in mice lacking the peroxisome proliferator-activated receptor  $\alpha$  (PPAR $\alpha$ ). *J. Biol. Chem.*, **273**, 5678-5684.
- Aoyama, T., Souri, M., Ueno, I., Kamijo, T., Yamaguchi, S., Rhead, W.J., Tanaka, K. & Hashimoto, T. (1995a) Cloning of human very-long-chain acyl-coenzyme A dehydrogenase and molecular characterization of its deficiency in two patients. *Am. J. Hum. Genet.*, **57**, 273-283.
- Aoyama, T., Souri, M., Ushikubo, S., Kamijo, T., Yamaguchi, S., Kelley, R.I., Rhead, W.J., Uetake, K., Tanaka, K. & Hashimoto, T. (1995b) Purification of human very-long-chain acyl-coenzyme A dehydrogenase and characterization of its deficiency in seven patients. *J. Clin. Invest.*, **95**, 2465-2473.
- Aoyama, T., Uchida, Y., Kelley, R.I., Marble, M., Hofman, K., Tongsgard, J.H., Rhead, W.J. & Hashimoto, T. (1993) A novel disease with deficiency of mitochondrial very-long-chain acyl-CoA dehydrogenase. *Biochem. Biophys. Res. Commun.*, **191**, 1369-1372.
- Aoyama, T., Ueno, I., Kamijo, T. & Hashimoto, T. (1994) Rat very-long-chain acyl-CoA dehydrogenase, a novel mitochondrial acyl-CoA dehydrogenase gene product, is a rate-limiting enzyme in long-chain fatty acid  $\beta$ -oxidation system. cDNA and deduced amino acid sequence and distinct specificities of the cDNA-expressed protein. *J. Biol. Chem.*, **269**, 19088-19094.
- Aoyama, T., Yamano, S., Waxman, D.J., Lapenson, D.P., Meyer, U.A., Fischer, V., Tyndale, R., Inaba, T., Kalow, W., Gelboin, H.V. & Gonzalez, F.J. (1989) Cytochrome P-450 hPCN3, a novel cytochrome P-450 IIIA gene product that is differentially expressed in adult human liver. cDNA and deduced amino acid sequence and distinct specificities of cDNA-expressed hpcn1 and hPCN3 for the metabolism of steroid hormones and cyclosporine. *J. Biol. Chem.*, **264**, 10388-10395.
- Baranowski, M., Błachnio, A., Zabielski, P. & Górski, J. (2007) PPAR $\alpha$  agonist induces the accumulation of ceramide in the heart of rats fed high-fat diet. *J. Physiol. Pharmacol.*, **58**, 57-72.
- Forman, B.M., Chen, J. & Evans, R.M. (1997) Hypolipidemic drugs, polyunsaturated fatty acids, and eicosanoids are ligands for peroxisome proliferator-activated receptors  $\alpha$  and  $\delta$ . *Proc. Natl. Acad. Sci. USA*, **94**, 4312-4317.
- Furuta, S., Miyazawa, S. & Hashimoto, T. (1981) Purification and properties of rat liver acyl-CoA dehydrogenases and electron transfer flavoprotein. *J. Biochem.*, **90**, 1739-1750.
- Gregersen, N., Andresen, B.S., Corydon, M.J., Corydon, T.J., Olsen, R.K., Bolund, L. & Bross, P. (2001) Mutation analysis in mitochondrial fatty acid oxidation defects: exemplified by acyl-CoA dehydrogenase deficiencies, with special focus on genotype-phenotype relationship. *Hum. Mutat.*, **18**, 169-189.
- Hanada, K. (2003) Serine palmitoyltransferase, a key enzyme of sphingolipid metabolism. *Biochim. Biophys. Acta*, **1632**, 16-30.
- Hu, R., Li, G., Kamijo, Y., Aoyama, T., Nakajima, T., Inoue, T., Node, K., Kannagi, R., Kyogashima, M. & Hara, A. (2007) Serum sulfatides as a novel biomarker for cardiovascular disease in patients with end-stage renal failure. *Glycoconj. J.*, **24**, 565-571.
- Izai, K., Uchida, Y., Orii, T., Yamamoto, S. & Hashimoto, T. (1992) Novel fatty acid  $\beta$ -oxidation enzymes in rat liver mitochondria. I. Purification and properties of very-long-chain acyl-coenzyme A dehydrogenase. *J. Biol. Chem.*, **267**, 1027-1033.
- Kamijo, Y., Hora, K., Kono, K., Takahashi, K., Higuchi, M., Ehara, T., Kiyosawa, K., Shigematsu, H., Gonzalez, F.J. & Aoyama, T. (2007) PPAR $\alpha$  protects proximal tubular cells from acute fatty acid toxicity. *J. Am. Soc. Nephrol.*, **18**, 3089-3100.
- Kanbe, H., Kamijo, Y., Nakajima, T., Tanaka, N., Sugiyama, E., Wang, L., Fang, Z.Z., Hara, A., Gonzalez, F.J. & Aoyama, T. (2014) Chronic ethanol consumption decreases serum sulfatide levels by suppressing hepatic cerebroside sulfotransferase expression in mice. *Arch. Toxicol.*, **88**, 367-379.
- Kehrer, J.P., Biswal, S.S., La, E., Thuillier, P., Datta, K., Fischer, S.M. & vanden Heuvel, J.P. (2001) Inhibition of peroxisome-proliferator-activated receptor (PPAR)  $\alpha$  by MK886. *Biochem. J.*, **356**, 899-906.
- Kimura, T., Nakajima, T., Kamijo, Y., Tanaka, N., Wang, L., Hara, A., Sugiyama, E., Tanaka, E., Gonzalez, F.J. & Aoyama, T. (2012) Hepatic cerebroside sulfotransferase is induced by PPAR $\alpha$  activation in mice. *PPAR Res.*, **2012**, 174932.
- Kliwer, S.A., Sundseth, S.S., Jones, S.A., Brown, P.J., Wisely, G.B., Koble, C.S., Devchand, P., Wahli, W., Willson, T.M., Lenhard, J.M. & Lehmann, J.M. (1997) Fatty acids and eicosanoids regulate gene expression through direct interactions with peroxisome proliferator-activated receptors  $\alpha$  and  $\gamma$ . *Proc. Natl. Acad. Sci. USA*, **94**, 4318-4323.
- Lehman, T.C., Hale, D.E., Bhala, A. & Thorpe, C. (1990) An acyl-coenzyme A dehydrogenase assay utilizing the ferrocenium ion. *Anal. Biochem.*, **186**, 280-284.
- Li, G., Hu, R., Kamijo, Y., Nakajima, T., Aoyama, T., Inoue, T., Node, K., Kannagi, R., Kyogashima, M. & Hara, A. (2007) Establishment of a quantitative, qualitative, and high-throughput analysis of sulfatides from small amounts of sera by matrix-assisted laser desorption ionization-time of flight mass spectrometry. *Anal. Biochem.*, **362**, 1-7.
- Nakajima, T., Elovaara, E., Gonzalez, F.J., Gelboin, H.V., Raunio, H., Pelkonen, O., Vainio, H. & Aoyama, T. (1994) Styrene metabolism by cDNA-expressed human hepatic and pulmonary cytochromes P450. *Chem. Res. Toxicol.*, **7**, 891-896.
- Nakajima, T., Kamijo, Y., Yuzhe, H., Kimura, T., Tanaka, N., Sugiyama, E., Nakamura, K., Kyogashima, M., Hara, A. & Aoyama, T. (2013) Peroxisome proliferator-activated receptor  $\alpha$  mediates enhancement of gene expression of cerebroside sulfotransferase in several murine organs. *Glycoconj. J.*, **30**, 553-560.
- Rivier, M., Castiel, I., Safonova, I., Ailhaud, G. & Michel, S. (2000) Peroxisome proliferator-activated receptor- $\alpha$  enhances lipid metabolism in a skin equivalent model. *J. Invest. Dermatol.*, **114**, 681-687.
- Souri, M., Aoyama, T., Orii, K., Yamaguchi, S. & Hashimoto, T. (1996) Mutation analysis of very-long-chain acyl-coenzyme A dehydrogenase (VLCAD) deficiency: identification and characterization of mutant VLCAD cDNAs from four patients. *Am. J. Hum. Genet.*, **58**, 97-106.
- Yamane, T., Kobayashi-Hattori, K. & Oishi, Y. (2011) A high-fat diet reduces ceramide synthesis by decreasing adiponectin levels and decreases lipid content by modulating HMG-CoA reductase and CPT-1 mRNA expression in the skin. *Mol. Nutr. Food Res.*, **55**, S186-S192.
- Zabielski, P., Błachnio-Zabielska, A., Baranowski, M., Zendzian-Piotrowska, M. & Gorski, J. (2010) Activation of PPAR $\alpha$  by bezafibrate negatively affects de novo synthesis of sphingolipids in regenerating rat liver. *Prostaglandins Other Lipid Mediat.*, **93**, 120-125.